Stochastic evaluation of second-order Dyson self-energies

Soohaeng Yoo Willow, Kwang S. Kim, and So Hirata

Articles you may be interested in

Stochastic evaluation of second-order many-body perturbation energies
The Journal of Chemical Physics **137**, 204122 (2012); 10.1063/1.4768697

Stochastic, real-space, imaginary-time evaluation of third-order Feynman–Goldstone diagrams
The Journal of Chemical Physics **140**, 024111 (2014); 10.1063/1.4861561

One-particle many-body Green's function theory: Algebraic recursive definitions, linked-diagram theorem, irreducible-diagram theorem, and general-order algorithms
The Journal of Chemical Physics **147**, 044108 (2017); 10.1063/1.4994837

Monte Carlo explicitly correlated second-order many-body perturbation theory
The Journal of Chemical Physics **145**, 154115 (2016); 10.1063/1.4964854

Stochastic multi-reference perturbation theory with application to the linearized coupled cluster method
The Journal of Chemical Physics **146**, 044107 (2017); 10.1063/1.4974177

Hybrid stochastic-deterministic calculation of the second-order perturbative contribution of multireference perturbation theory
The Journal of Chemical Physics **147**, 034101 (2017); 10.1063/1.4992127

Stochastic evaluation of second-order Dyson self-energies

Soohaeng Yoo Willow,[1,2,3] Kwang S. Kim,[2] and So Hirata[1,3,a]

[1]*Department of Chemistry, University of Illinois at Urbana-Champaign, 600 South Mathews Avenue, Urbana, Illinois 61801, USA*
[2]*Center for Superfunctional Materials, Department of Chemistry, Pohang University of Science and Technology, San 31, Hyojadong, Namgu, Pohang 790-784, Korea*
[3]*CREST, Japan Science and Technology Agency, 4-1-8 Honcho, Kawaguchi, Saitama 332-0012, Japan*

A stochastic method is proposed that evaluates the second-order perturbation corrections to the Dyson self-energies of a molecule (i.e., quasiparticle energies or correlated ionization potentials and electron affinities) directly and not as small differences between two large, noisy quantities. With the aid of a Laplace transform, the usual sum-of-integral expressions of the second-order self-energy in many-body Green's function theory are rewritten into a sum of just four 13-dimensional integrals, 12-dimensional parts of which are evaluated by Monte Carlo integration. Efficient importance sampling is achieved with the Metropolis algorithm and a 12-dimensional weight function that is analytically integrable, is positive everywhere, and cancels all the singularities in the integrands exactly and analytically. The quasiparticle energies of small molecules have been reproduced within a few mE_h of the correct values with 10^8 Monte Carlo steps. Linear-to-quadratic scaling of the size dependence of computational cost is demonstrated even for these small molecules. © *2013 AIP Publishing LLC*. [http://dx.doi.org/10.1063/1.4801862]

I. INTRODUCTION

Recently, we proposed a stochastic method of evaluating the second-order Møller–Plesset perturbation (MP2) correction to the Hartree–Fock (HF) energy of a molecule.[1] The MP2 energy has two diagrammatic contributions (Fig. 1),

$$E^{(2)} = E^{(A)} + E^{(B)}, \tag{1}$$

each of which is the fourfold summation of products of two 6-dimensional integrals,

$$E^{(A)} = 2 \sum_{i,j}^{\mathrm{occ.}} \sum_{a,b}^{\mathrm{vir.}} \frac{\langle ij|ab \rangle \langle ab|ij \rangle}{\epsilon_i + \epsilon_j - \epsilon_a - \epsilon_b}, \tag{2}$$

$$E^{(B)} = -\sum_{i,j}^{\mathrm{occ.}} \sum_{a,b}^{\mathrm{vir.}} \frac{\langle ij|ab \rangle \langle ab|ji \rangle}{\epsilon_i + \epsilon_j - \epsilon_a - \epsilon_b}, \tag{3}$$

where ϵ_p is the pth orbital energy of the HF theory and $\langle ij|ab \rangle$ is a two-electron integral[2] over occupied (labeled by i and j) and virtual (a and b) molecular orbitals (MO's),

$$\langle ij|ab \rangle = \int d\boldsymbol{r}_1 \int d\boldsymbol{r}_2 \frac{\varphi_i^*(\boldsymbol{r}_1)\varphi_j^*(\boldsymbol{r}_2)\varphi_a(\boldsymbol{r}_1)\varphi_b(\boldsymbol{r}_2)}{r_{12}}, \tag{4}$$

with $r_{12} = |\boldsymbol{r}_1 - \boldsymbol{r}_2|$. Using a Laplace transform,[3]

$$\frac{1}{\epsilon_i + \epsilon_j - \epsilon_a - \epsilon_b} = -\int_0^\infty d\tau \exp\{(\epsilon_i + \epsilon_j - \epsilon_a - \epsilon_b)\tau\}, \tag{5}$$

the above canonical expressions are converted into single 13-dimensional integrals,

$$E^{(A)} = -2 \int d\boldsymbol{r}_1 \int d\boldsymbol{r}_2 \int d\boldsymbol{r}_3 \int d\boldsymbol{r}_4 \int_0^\infty d\tau$$
$$\times \frac{o(\boldsymbol{r}_1, \boldsymbol{r}_3, \tau)o(\boldsymbol{r}_2, \boldsymbol{r}_4, \tau)v(\boldsymbol{r}_1, \boldsymbol{r}_3, \tau)v(\boldsymbol{r}_2, \boldsymbol{r}_4, \tau)}{r_{12}r_{34}}, \tag{6}$$

$$E^{(B)} = \int d\boldsymbol{r}_1 \int d\boldsymbol{r}_2 \int d\boldsymbol{r}_3 \int d\boldsymbol{r}_4 \int_0^\infty d\tau$$
$$\times \frac{o(\boldsymbol{r}_1, \boldsymbol{r}_4, \tau)o(\boldsymbol{r}_2, \boldsymbol{r}_3, \tau)v(\boldsymbol{r}_1, \boldsymbol{r}_3, \tau)v(\boldsymbol{r}_2, \boldsymbol{r}_4, \tau)}{r_{12}r_{34}}, \tag{7}$$

with

$$o(\boldsymbol{r}_1, \boldsymbol{r}_3, \tau) = \sum_i^{\mathrm{occ.}} \varphi_i^*(\boldsymbol{r}_1)\varphi_i(\boldsymbol{r}_3) \exp(\epsilon_i \tau), \tag{8}$$

$$v(\boldsymbol{r}_1, \boldsymbol{r}_3, \tau) = \sum_a^{\mathrm{vir.}} \varphi_a(\boldsymbol{r}_1)\varphi_a^*(\boldsymbol{r}_3) \exp(-\epsilon_a \tau), \tag{9}$$

where φ_p is the pth HF MO. In our Monte Carlo MP2 (MC-MP2), the 12-dimensional parts ($\boldsymbol{r}_1$, $\boldsymbol{r}_2$, $\boldsymbol{r}_3$, and $\boldsymbol{r}_4$) of Eqs. (6) and (7) are evaluated by MC integration using four-electron walkers wandering in 12-dimensional real space. Importance sampling is essential.[1]

As compared to the conventional implementations of MP2, MC-MP2 has a vastly lower scaling of cost with system size and a far smaller memory requirement.[1] The price one pays is the introduction of statistical errors, which
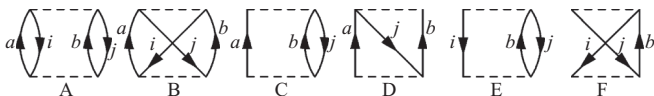
a)sohirata@illinois.edu

FIG. 1. Goldstone diagrams for the second-order corrections to the energy (A and B) and self-energy (C through F).

decay as the inverse square root of the number of MC steps. This method is also expected to be easily extensible to more complex theories, such as explicitly correlated MP2 (Refs. 4 and 5) and higher-order perturbation corrections, and well suited to massive parallelism. Regarding the latter issue, the architectures of modern supercomputers with hundreds of thousands or even millions of processors are forcing the conventional algorithms of many-body theories (which are dominated by matrix algebra and, therefore, fundamentally nonscalable) to be redesigned into forms that are naturally parallel. MC-MP2 is an example of such redesign.

MC-MP2 can also be viewed as a new branch of quantum Monte Carlo (QMC).[6–12] It has a number of characteristics not seen in any existing incarnations of QMC. (1) MC-MP2 directly computes correlation energies, leaving the much greater HF contribution to the usual deterministic algorithm. This is in contrast to most QMC methods, which usually must compute the whole energy by stochastic algorithms with concomitant errors, the majority of which are associated with the HF part. (2) It does not suffer from the fixed-node errors of diffusion MC and is guaranteed to converge at the exact MP2 energy. (3) It is also distinguished from the stochastic perturbation theory of Thom and Alavi[13] or the fast stochastic MP2 of Neuhauser *et al.*[14] In the former, walkers explore high-dimensional Hilbert space with the assumption that MO integrals, $\langle ij|ab\rangle$, are readily available. In the latter, (imaginary) time-dependent orbitals are introduced, which are generated by a stochastic algorithm. However, the evaluation of the two-electron integrals for these orbitals seems to be done by the conventional way; in Ref. 14, semi-empirical approximations to these integrals have been used. With the *ab initio* Hamiltonian, there is hardly any computational advantage in these methods over the conventional MP2 because the transformation and storage of these integrals are the operation and memory hotspots. In MC-MP2, in contrast, both are completely eliminated.[1]

Another important expected advantage of MC-MP2 over other QMC methods is that (4) properties other than the total ground-state energies can be evaluated directly and neither as small differences between two large quantities with statistical errors nor as numerical derivatives of noisy functions. The objective of this study is to demonstrate this advantage in the case of second-order Dyson self-energy in many-body Green's function theory.[15–17] The self-energy gives correlated one-electron energies (ionization potentials and electron affinities) in a molecule and quasiparticle energy bands in a crystalline solid.[18–25] The significance of accurate one-electron energies and energy bands needs no explanation, but the perturbation expansion of the self-energy, which can systematically improve these quantities, does not easily lend itself to usual QMC treatments. Here, we show that MC-MP2

can compute them in a molecule stochastically, efficiently, and accurately.

II. THEORY

The second-order Dyson self-energy has four diagrammatic contributions (Fig. 1). In the diagonal approximation,[16] the correlated one-electron energy of the pth orbital is given by

$$\epsilon_p^{(2)} = \epsilon_p + \Sigma_p^{(C)}(\epsilon_p) + \Sigma_p^{(D)}(\epsilon_p) + \Sigma_p^{(E)}(\epsilon_p) + \Sigma_p^{(F)}(\epsilon_p),$$
(10)

with

$$\Sigma_p^{(C)}(\omega) = 2 \sum_j^{\text{occ.}} \sum_{a,b}^{\text{vir.}} \frac{\langle pj|ab\rangle\langle ab|pj\rangle}{\omega + \epsilon_j - \epsilon_a - \epsilon_b},$$
(11)

$$\Sigma_p^{(D)}(\omega) = -\sum_j^{\text{occ.}} \sum_{a,b}^{\text{vir.}} \frac{\langle jp|ab\rangle\langle ab|pj\rangle}{\omega + \epsilon_j - \epsilon_a - \epsilon_b},$$
(12)

$$\Sigma_p^{(E)}(\omega) = -2 \sum_{i,j}^{\text{occ.}} \sum_b^{\text{vir.}} \frac{\langle ij|pb\rangle\langle pb|ij\rangle}{\epsilon_i + \epsilon_j - \omega - \epsilon_b},$$
(13)

$$\Sigma_p^{(F)}(\omega) = \sum_{i,j}^{\text{occ.}} \sum_b^{\text{vir.}} \frac{\langle ji|pb\rangle\langle pb|ij\rangle}{\epsilon_i + \epsilon_j - \omega - \epsilon_b},$$
(14)

where ω is approximated by ϵ_p in Eq. (10). Using the Laplace transform [Eq. (5)], which allows the order of summation and integration to be changed, we can rewrite these sum-of-integral expressions into single 13-dimensional integrals,

$$\Sigma_p^{(C)}(\omega) = -2 \int d\mathbf{r}_1 \int d\mathbf{r}_2 \int d\mathbf{r}_3 \int d\mathbf{r}_4 \int_0^\infty d\tau$$
$$\times \frac{p(\mathbf{r}_1,\mathbf{r}_3,\tau)o(\mathbf{r}_2,\mathbf{r}_4,\tau)v(\mathbf{r}_1,\mathbf{r}_3,\tau)v(\mathbf{r}_2,\mathbf{r}_4,\tau)}{r_{12}r_{34}},$$
(15)

$$\Sigma_p^{(D)}(\omega) = \int d\mathbf{r}_1 \int d\mathbf{r}_2 \int d\mathbf{r}_3 \int d\mathbf{r}_4 \int_0^\infty d\tau$$
$$\times \frac{o(\mathbf{r}_1,\mathbf{r}_4,\tau)p(\mathbf{r}_2,\mathbf{r}_3,\tau)v(\mathbf{r}_1,\mathbf{r}_3,\tau)v(\mathbf{r}_2,\mathbf{r}_4,\tau)}{r_{12}r_{34}},$$
(16)

$$\Sigma_p^{(E)}(\omega) = 2 \int d\mathbf{r}_1 \int d\mathbf{r}_2 \int d\mathbf{r}_3 \int d\mathbf{r}_4 \int_0^\infty d\tau$$
$$\times \frac{o(\mathbf{r}_1,\mathbf{r}_3,\tau)o(\mathbf{r}_2,\mathbf{r}_4,\tau)\tilde{p}(\mathbf{r}_1,\mathbf{r}_3,\tau)v(\mathbf{r}_2,\mathbf{r}_4,\tau)}{r_{12}r_{34}},$$
(17)

$$\Sigma_p^{(F)}(\omega) = -\int d\mathbf{r}_1 \int d\mathbf{r}_2 \int d\mathbf{r}_3 \int d\mathbf{r}_4 \int_0^\infty d\tau$$
$$\times \frac{o(\mathbf{r}_1,\mathbf{r}_4,\tau)o(\mathbf{r}_2,\mathbf{r}_3,\tau)\tilde{p}(\mathbf{r}_1,\mathbf{r}_3,\tau)v(\mathbf{r}_2,\mathbf{r}_4,\tau)}{r_{12}r_{34}},$$
(18)

with

$$p(\boldsymbol{r}_1, \boldsymbol{r}_3, \tau) = \varphi_p^*(\boldsymbol{r}_1)\varphi_p(\boldsymbol{r}_3)\exp(\omega\tau), \qquad (19)$$

$$\tilde{p}(\boldsymbol{r}_1, \boldsymbol{r}_3, \tau) = \varphi_p(\boldsymbol{r}_1)\varphi_p^*(\boldsymbol{r}_3)\exp(-\omega\tau). \qquad (20)$$

Note that the Laplace-transformed expressions of Eqs. (11)–(14) can be obtained, alternatively and directly, by applying the interpretation rules of time-domain Green's functions[15] to the open diagrams in Fig. 1.

In this work, we evaluate the 12-dimensional integration over four electron coordinates ($\boldsymbol{r}_1$ through $\boldsymbol{r}_4$) in Eqs. (15)–(18) using MC. The remaining one-dimensional integration over τ is done with a 21-point Gauss–Kronrod quadrature.[1,26] This scheme, therefore, inherits all the aforementioned advantages and disadvantages of MC-MP2 for energies.

The MC integration[27] of each of Eqs. (15)–(18) can be understood in a unified way as the following approximation:

$$I = \int d\boldsymbol{r}_1 \int d\boldsymbol{r}_2 \int d\boldsymbol{r}_3 \int d\boldsymbol{r}_4 \int_0^\infty d\tau$$
$$\times f(\boldsymbol{r}_1, \boldsymbol{r}_2, \boldsymbol{r}_3, \boldsymbol{r}_4, \tau) \qquad (21)$$

$$\approx \frac{1}{N}\sum_{n=1}^{N}\sum_{q=1}^{21} \frac{w_q f\left(\boldsymbol{r}_1^{[n]}, \boldsymbol{r}_2^{[n]}, \boldsymbol{r}_3^{[n]}, \boldsymbol{r}_4^{[n]}, \tau_q\right)}{w\left(\boldsymbol{r}_1^{[n]}, \boldsymbol{r}_2^{[n]}, \boldsymbol{r}_3^{[n]}, \boldsymbol{r}_4^{[n]}\right)}, \qquad (22)$$

where N is the number of MC steps or sampling points of four-electron walkers, whose positions in the real space are given by ($\boldsymbol{r}_1^{[n]}, \boldsymbol{r}_2^{[n]}, \boldsymbol{r}_3^{[n]}, \boldsymbol{r}_4^{[n]}$), and τ_q and w_q are Gauss–Kronrod quadrature points and weights,[1] respectively. The sampling points are distributed randomly but according to the 12-dimensional weight function $w(\boldsymbol{r}_1, \boldsymbol{r}_2, \boldsymbol{r}_3, \boldsymbol{r}_4)$ and this distribution is achieved by the Metropolis–Rosenbluth–Rosenbluth–Teller–Teller algorithm.[28]

The key to high efficiency in MC integrations lies in finding a suitable weight function,[27] in this case, $w(\boldsymbol{r}_1, \boldsymbol{r}_2, \boldsymbol{r}_3, \boldsymbol{r}_4)$. It must be analytically integrable,

$$\int d\boldsymbol{r}_1 \int d\boldsymbol{r}_2 \int d\boldsymbol{r}_3 \int d\boldsymbol{r}_4 w(\boldsymbol{r}_1, \boldsymbol{r}_2, \boldsymbol{r}_3, \boldsymbol{r}_4) = 1, \quad (23)$$

be positive everywhere,

$$w(\boldsymbol{r}_1, \boldsymbol{r}_2, \boldsymbol{r}_3, \boldsymbol{r}_4) > 0, \qquad (24)$$

cancel all singularities in the integrands exactly and analytically,

$$\left|\frac{f(\boldsymbol{r}_1, \boldsymbol{r}_2, \boldsymbol{r}_3, \boldsymbol{r}_4, \tau_q)}{w(\boldsymbol{r}_1, \boldsymbol{r}_2, \boldsymbol{r}_3, \boldsymbol{r}_4)}\right| < \infty \qquad (25)$$

and generally behave like $f(\boldsymbol{r}_1, \boldsymbol{r}_2, \boldsymbol{r}_3, \boldsymbol{r}_4, \tau_q)$ so that the quotient f/w is a smooth function throughout the domain of integration. Note that all of the integrands in Eqs. (15)–(18) have singularities at $r_{12} = 0$ and $r_{34} = 0$, i.e., everywhere in the 12-dimensional real space.

We use the following weight function, which has been successful for MC-MP2 for energies:[1]

$$w(\boldsymbol{r}_1, \boldsymbol{r}_2, \boldsymbol{r}_3, \boldsymbol{r}_4) = \frac{1}{E_g^2} \frac{g(\boldsymbol{r}_1)g(\boldsymbol{r}_2)g(\boldsymbol{r}_3)g(\boldsymbol{r}_4)}{r_{12}r_{34}}, \quad (26)$$

where $g(\boldsymbol{r})$ is a sum of s-type Gaussian functions centered at constituent atoms and

$$E_g = \int d\boldsymbol{r}_1 \int d\boldsymbol{r}_2 \frac{g(\boldsymbol{r}_1)g(\boldsymbol{r}_2)}{r_{12}}. \qquad (27)$$

The right-hand side can be evaluated analytically.[29]

In MC-MP2, sampling points ($\boldsymbol{r}_1^{[n]}, \boldsymbol{r}_2^{[n]}, \boldsymbol{r}_3^{[n]}, \boldsymbol{r}_4^{[n]}$) with $n = 1, \ldots, N$ are generated according to this weight function by the Metropolis algorithm. At each point, we evaluate the values of $o(\boldsymbol{r}_i, \boldsymbol{r}_j, \tau_q)$ [Eq. (8)], $v(\boldsymbol{r}_i, \boldsymbol{r}_j, \tau_q)$ [Eq. (9)], $p(\boldsymbol{r}_i, \boldsymbol{r}_j, \tau_q)$ [Eq. (19)], and $\tilde{p}(\boldsymbol{r}_i, \boldsymbol{r}_j, \tau_q)$ [Eq. (20)] at all τ_q's ($q = 1, \ldots, 21$) as well as the weight function $w(\boldsymbol{r}_1, \boldsymbol{r}_2, \boldsymbol{r}_3, \boldsymbol{r}_4)$. Using them, we add contributions from the point to the approximate values of the right-hand sides of Eqs. (15)–(18). Hence, a single MC run informs all four diagrammatic contributions at all 21 grid points, $\{\tau_q\}$. For a fixed value of N, the cost of MC-MP2 is determined by that of evaluating all MO amplitudes at a sampling point, which in turn consists in calculating all atomic orbital (AO) amplitudes and summing them to obtain MO amplitudes. The cost is, therefore, proportional to the number of MO's (m) times the number of AO's (m) and grows quadratically with size [$O(m^2)$]. In practice, since calculating AO amplitudes is far more expensive than summing them, the actual cost is expected to display near-linear [$O(m)$] size dependence. This superior cost scaling of MC-MP2 comes with inevitable statistical errors.

III. RESULTS AND DISCUSSION

Table I compares the second-order Dyson self-energies (i.e., the correlation corrections to one-electron energies) for the highest occupied MO's (HOMO's) and lowest unoccupied MO's (LUMO's) of N_2, O_2, H_2O, CH_4, and C_2H_6 obtained by MC-MP2 and conventional MP2. With either method, the inverse Dyson equation was not solved self-consistently; the self-energies were evaluated with $\omega = \epsilon_p$.[16] As seen, the MC algorithm can reproduce the correct values within a few mE_h after 10^8 steps. These statistical errors are smaller than both the magnitudes of the correlation

TABLE I. The second-order Dyson self-energies (in E_h) for HOMO and LUMO of various molecules evaluated by the conventional and MC methods of MP2/6-31G** (frozen core).

Molecule	Method	HOMO	LUMO
N_2[a]	MP2 (conventional)	-0.0721	0.0005
N_2[a]	MC-MP2 ($N = 10^8$)	-0.0725	0.0006
O_2[b]	MP2 (conventional)	0.1287	-0.0360
O_2[b]	MC-MP2 ($N = 10^8$)	0.1291	-0.0335
H_2O[c]	MP2 (conventional)	0.1036	-0.0230
H_2O[c]	MC-MP2 ($N = 10^8$)	0.1051	-0.0236
CH_4[d]	MP2 (conventional)	0.0330	-0.0311
CH_4[d]	MC-MP2 ($N = 10^8$)	0.0339	-0.0340
C_2H_6[e]	MP2 (conventional)	0.0367	-0.0357
C_2H_6[e]	MC-MP2 ($N = 10^8$)	0.0377	-0.0446

[a]NN distance: 1.420 Å.
[b]OO distance: 1.200 Å.
[c]OH distance: 0.961 Å; HOH angle: 103.826°.
[d]CH distance: 1.087 Å.
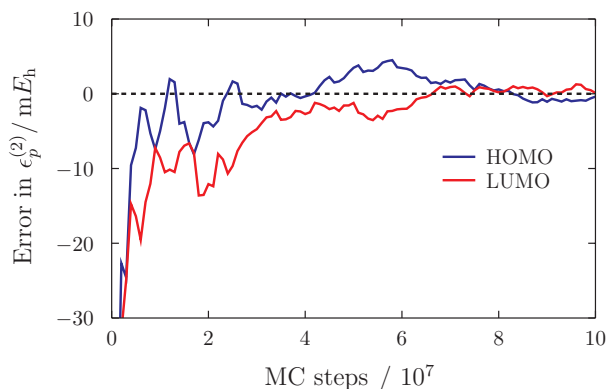[e]CC distance: 1.523 Å; CH distance: 1.089 Å; HCC angle: 111.189°.

FIG. 2. The errors in $\epsilon_p^{(2)}$ (in mE_h) for HOMO and LUMO of N_2 evaluated by MC-MP2/6-31G** (frozen core) as a function of the number of MC steps.

FIG. 4. The same as Fig. 3, but for virtual orbitals.

corrections and typical precisions (0.1 eV) of measurements of such quantities. Figure 2 shows the convergence of these results with the MC steps for N_2. Note that $\epsilon_p^{(2)}$ plotted here are *integrated* quantities [Eq. (22)] and not some instantaneous quantities calculable with just the existing walkers at a given MC step.

For these calculations, we have used the following weight functions:

$$g_{N_2}(\boldsymbol{r}) = \sum_{N=1}^{2} g_N(\boldsymbol{r}), \tag{28}$$

$$g_{O_2}(\boldsymbol{r}) = \sum_{O=1}^{2} g_O(\boldsymbol{r}), \tag{29}$$

$$g_{H_2O}(\boldsymbol{r}) = 6g_O(\boldsymbol{r}) + \sum_{H=1}^{2} g_H(\boldsymbol{r}), \tag{30}$$

$$g_{C_nH_m}(\boldsymbol{r}) = \sum_{C=1}^{n} 4g_C(\boldsymbol{r}) + \sum_{H=1}^{m} g_H(\boldsymbol{r}), \tag{31}$$

with

$$g_A(\boldsymbol{r}) = \exp\left(-\zeta_1 r_A^2\right) + 0.1\exp\left(-\zeta_2 r_A^2\right), \tag{32}$$

where r_A is the distance from atom A and $(\zeta_1, \zeta_2) = (0.6, 0.15)$ for H, $(0.5, 0.1)$ for C, $(0.6, 0.1)$ for N, and $(0.8, 0.2)$ for O. The prefactors of 6 and 4 in Eqs. (30) and (31) are the numbers of valence electrons in the respective atoms.
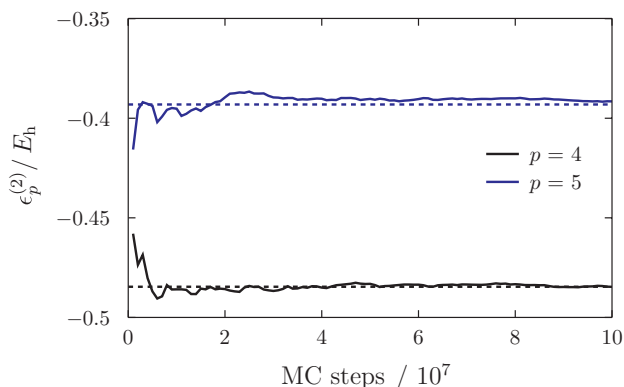
The correlation corrections to the orbital energies of HOMO (LUMO) can in principle be calculated by existing QMC methods by taking differences in correlated total energy between the neutral and cation (anion) species, which need to be separately evaluated. We have already mentioned that MC-MP2 has the distinct advantage over such a scheme by being able to compute those quantities directly not as small differences of large, noisy quantities. In addition, MC-MP2 for self-energies is not limited to HOMO or LUMO; it can yield correlated one-electron energies of all orbitals or any subset thereof (some of which are subject to instabilities[24,25] unrelated to the algorithm itself) from a single MC run. Figures 3 and 4 plot the correlated one-electron energies, $\epsilon_p^{(2)}$, for $p = 4$ through 7 of H_2O ($p = 5$ and 6 are HOMO and LUMO, respectively) as a function of the number of MC steps. They also underscore the rapid convergence and smallness of the statistical errors relative to the absolute values of the orbital energies. The plot suggests that MC-MP2 is sufficiently reliable with a tenth of the number of MC steps carried out for these plots.

Figure 5 plots the operation cost of the MC-MP2 self-energy calculations of four orbitals of each of the five molecules in Table I as a function of the number of MO's (m). The measured cost displays the size dependence in

FIG. 3. $\epsilon_p^{(2)}$ (in E_h) of occupied orbitals of H_2O evaluated by MC-MP2/6-31G** (frozen core) as a function of the number of MC steps.
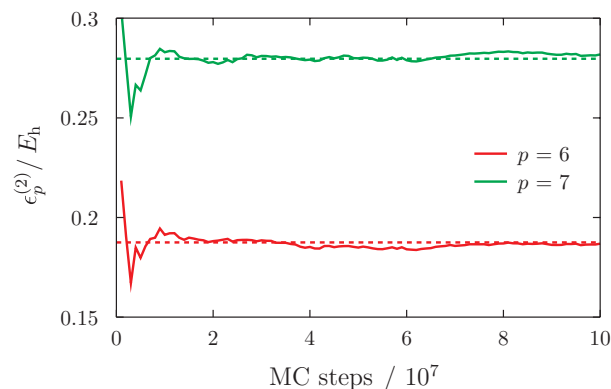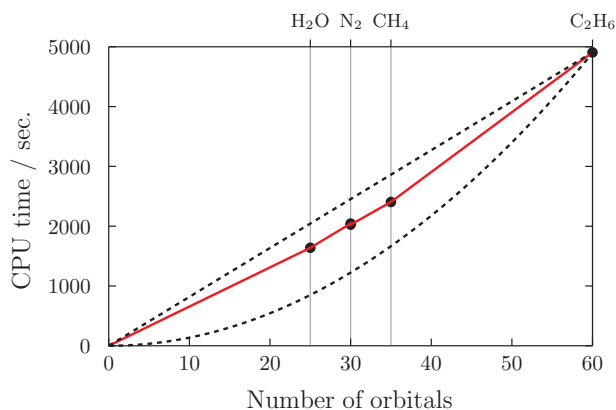

FIG. 5. The CPU time (in s) spent by the MC-MP2 ($N = 10^8$) calculations as a function of the number of MO's (m). The dashed line and curve are linear and quadratic functions of m to guide the eyes. The plot for O_2 is indistinguishable from that of N_2.

between linear and quadratic, as anticipated from the foregoing discussion on the algorithms. This may be contrasted with the $O(m^5)$ dependence of the cost of conventional MP2 for energies or self-energies. Even though the prefactor multiplying the cost function is still large in MC-MP2, considering the near-linear scaling of cost increase with size, the negligibly small memory requirement, and the naturally parallel algorithm with virtually no interprocessor communication needs, we believe that MC-MP2 is the future of MP2.

ACKNOWLEDGMENTS

[1] S. Y. Willow, K. S. Kim, and S. Hirata, J. Chem. Phys. **137**, 204122 (2012).
[2] I. Shavitt and R. J. Bartlett, *Many-Body Methods in Chemistry and Physics* (Cambridge University Press, Cambridge, 2009).
[3] J. Almlöf, Chem. Phys. Lett. **181**, 319 (1991).
[4] S. Ten-no, J. Chem. Phys. **121**, 117 (2004).
[5] T. Shiozaki, E. F. Valeev, and S. Hirata, Annu. Rep. Comp. Chem. **5**, 131 (2009).
[6] D. M. Ceperley and B. J. Alder, Phys. Rev. Lett. **45**, 566 (1980).
[7] B. L. Hammond, W. A. Lester, Jr., and P. J. Reynolds, *Monte Carlo Methods in Ab Initio Quantum Chemistry* (World Scientific, Singapore, 1994).
[8] A. Luchow and J. B. Anderson, Annu. Rev. Phys. Chem. **51**, 501 (2000).
[9] J. Kolorenč and L. Mitas, Rep. Prog. Phys. **74**, 026502 (2011).
[10] R. Blankenbecler, D. J. Scalapino, and R. L. Sugar, Phys. Rev. D **24**, 2278 (1981).
[11] G. Sugiyama and S. E. Koonin, Ann. Phys. **168**, 1 (1986).
[12] S. Zhang and H. Krakauer, Phys. Rev. Lett. **90**, 136401 (2003).
[13] A. J. W. Thom and A. Alavi, Phys. Rev. Lett. **99**, 143001 (2007).
[14] D. Neuhauser, E. Rabani, and R. Baer, J. Chem. Theory Comput. **9**, 24 (2013).
[15] R. D. Mattuck, *A Guide to Feynman Diagrams in the Many-Body Problem* (Dover, New York, 1992).
[16] A. Szabo and N. S. Ostlund, *Modern Quantum Chemistry* (Dover, New York, 1996).
[17] J. V. Ortiz, Adv. Quantum Chem. **35**, 33 (1999).
[18] A. B. Kunz, Phys. Rev. B **6**, 606 (1972).
[19] D. P. Chong, F. G. Herring, and D. McWilliams, J. Chem. Phys. **61**, 78 (1974).
[20] V. Kvasnička and I. Hubač, J. Chem. Phys. **60**, 4483 (1974).
[21] S. Pantelides, D. Mickish, and A. Kunz, Phys. Rev. B **10**, 2602 (1974).
[22] J. Paldus and J. Cizek, Adv. Qauntum Chem. **9**, 105 (1975).
[23] S. Suhai, Phys. Rev. B **27**, 3506 (1983).
[24] J.-Q. Sun and R. J. Bartlett, J. Chem. Phys. **104**, 8553 (1996).
[25] S. Hirata and R. J. Bartlett, J. Chem. Phys. **112**, 7339 (2000).
[26] A. S. Kronrod, *Nodes and Weights of Quadrature Formulas. Sixteen-Place Tables* (Consultants Bureau, New York, 1965).
[27] M. H. Kalos and P. A. Whitlock, *Monte Carlo Methods* (Wiley-VCH, Weinheim, 2008).
[28] N. Metropolis, A. W. Rosenbluth, M. N. Rosenbluth, A. N. Teller, and E. Teller, J. Chem. Phys. **21**, 1087 (1953).
[29] S. Obara and A. Saika, J. Chem. Phys. **84**, 3963 (1986).